10 Large roofs and sports stadiums

10.1 Introduction

Wind loading is usually the dominant structural loading on the roofs of large buildings, such as entertainment or exhibition centres, closed or partially-closed sports buildings, aircraft hangars, etc. The wind loads on these structures have some significant differences in comparison with those on the roofs of smaller low-rise buildings, that justifies separate treatment:

- The quasi-steady approach (Section 4.6.2), although appropriate for small buildings, is not applicable for large roofs
- Resonant effects, although not dominant, can be significant

These roofs are commonly of low pitch, and experience large areas of attached flow, with low correlations between the pressure fluctuations acting on different parts. Downward as well as upward external pressures can be significant. These roofs are often arched or domed structures, which are sensitive to the distributions of wind loads, and the possibility of critical 'unbalanced' pressure distributions should be considered.

This chapter will first consider the aerodynamic aspects of wind flow over large roofs, which will facilitate an understanding of the steady and fluctuating components of wind pressures acting on these structures. Then methods of obtaining design wind loads are described, with emphasis on the method of effective static wind-load distributions, introduced in earlier chapters. The incorporation of resonant contributions is also discussed.

10.2 Wind flow over large roofs

Figure 8.5 in Chapter 8 shows the main features of the flow over a low-pitched roof, with the wind blowing normal to one wall. At the top of the windward wall, the flow 'separates' and 're-attaches' further along the roof, forming a separation 'bubble'. The turbulence in the wind flow plays an important role in determining the length of the separation bubble – high turbulence gives a shorter bubble length, low turbulence produces a longer bubble. Even in open country turbulence intensities in windstorms are equal to 10–20% of the mean or slowly varying wind speed, and in this situation mean separation bubble lengths are equal to two to three wall heights.

The separation bubble region is a very important one for large roofs because the upwards pressures are the greatest in this region. In the re-attached flow region, the pressures are quite small. Thus for very large flat or near-flat roofs, only the edge regions within two to three wall heights from the edge will experience large pressures, and large areas of the roof will experience quite low pressures. The variation of mean uplift pressures, measured in some wind tunnel tests (Davenport and Surry, 1974) for flat roofs, shown in Figure

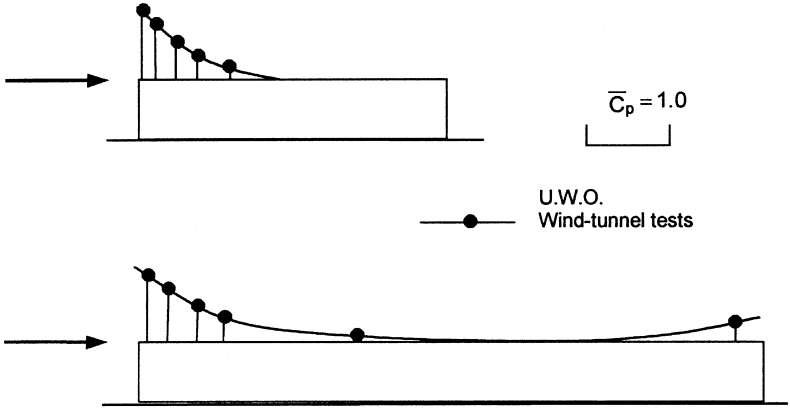

Figure 10.1 Mean pressure distributions on flat roofs.

10.1, illustrate this point. It should be noted that fluctuations in pressures occur so that downwards as well as upwards pressures can occur for short time periods. Not all codes or standards on wind loads specify these downwards pressure coefficients, as discussed in Chapter 15.

As the roof pitch increases, the point of flow separation moves away from the leading edge of the roof and, in the case of a curved or arched roof, separation usually occurs downstream of the apex (Figure 10.2, from Blessmann, 1991). Upwind of the separation point, the pressures may be downwards (positive) or upwards (negative) near the leading edge, depending on the rise to span ratio, but are always upwards at the apex. Downwind of the separation point they are upwards with small magnitudes.

The form of the net mean pressure coefficient distribution (i.e. the top surface pressure minus the bottom surface pressure) on a large cantilevered stadium roof is shown in Figure 10.3. Negative values indicate net upwards pressure differences. The largest uplift occurs at the leading edge, and reduces to a small pressure difference at the rear. The top surface experiences flow separation, so that the characteristic pressure distribution peaks at the leading edge, and reduces quite rapidly downstream. Underneath the flow stagnates at the back of the grandstand, if there is no gap present, to reach a pressure approaching the dynamic pressure of the freestream. However, the underside pressure will reduce in magnitude with increasing vent gaps at the back of the grandstand.

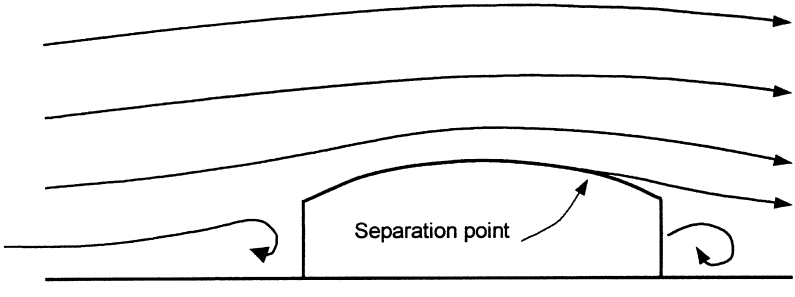

Figure 10.2 Flow separations over arched roofs (from Blessmann, 1991).

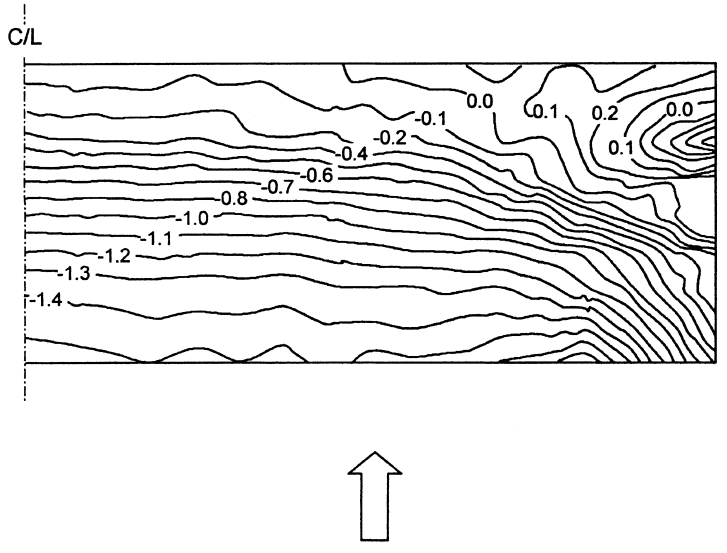

Figure 10.3 Mean net pressure distributions on a cantilevered stadium roof (Lam and To, 1995).

10.3 Arched and domed roofs

Arched roofs are structurally efficient, and are popular for structures like aircraft hangars, and enclosed sports arenas, which require large clear spans. Figure 10.4 shows the geo-

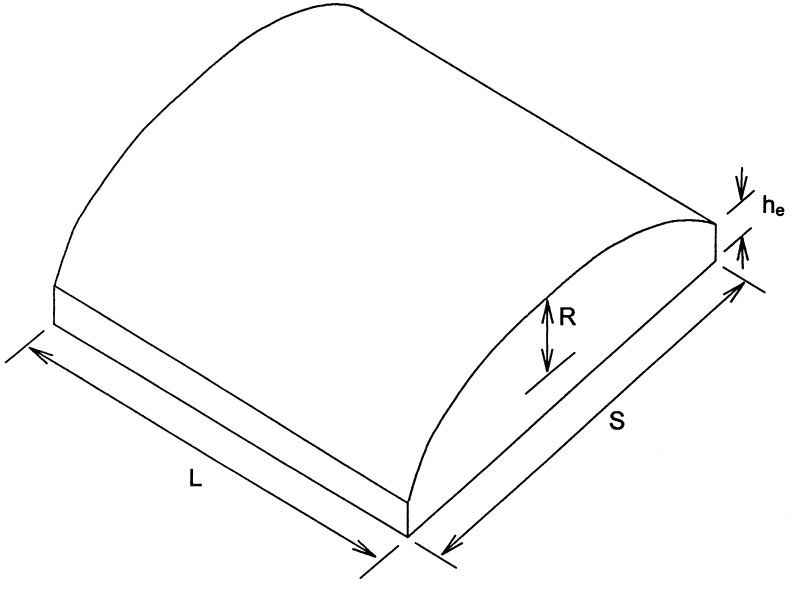

Figure 10.4 Geometric parameters for arched roof buildings.

metric variables that are relevant to the wind loading of arched-roof buildings. The variables are: the span, S; the length, L; the rise, R; the height of the walls to the eaves level, h_e.

Some very early studies on arched roofs were carried out in an aeronautical wind tunnel in the Soviet Union in the 1920s (Bounkin and Tcheremoukhin, 1928). These data found their way into a number of national codes and standards on wind loading, and are still widely used at the present day, after reference by the American Society of Civil Engineers (1936). Some early full-scale measurements on the Akron Airship Hangar, which had an arched roof of high rise-to-span ratio, were described by Arnstein and Klemperer (1936).

Arched roofs were apparently given very little attention by researchers after 1936 until the 1980s. Grillaud (1981) described full-scale studies of wind loads on an inflatable structure, and Hoxey and Richardson (1983) also measured full-scale loads on film plastic greenhouses. These structures both had rise/span ratios of 0.5. Holmes (1984) carried out wind tunnel measurements on a single aircraft hangar model with a rise/span ratio (R/S) of 0.20. Although the latter tests were carried out at low Reynolds numbers, the curved roof surface was roughened. The effect of a ridge ventilator on the apex of the roof was also investigated and found to be significant. A significant aspect of the latter work was an early attempt to establish effective static load distributions for load effects, such as axial forces and bending moments in the arch.

Johnson *et al*. (1985) reviewed existing model and full-scale data, and described some new wind tunnel results from the University of Western Ontario. They found significant Reynolds number effects in their wind tunnel data for models with a rise/span ratio of 0.5.

Toy and Tahouri (1988) carried out measurements on models of semi-cylindrical structures ($R/S = 0.5$; $h_e/R = 0$). These wind tunnel measurements were carried out with a smooth-wall boundary flow (very high Jensen number – see Section 4.4.5), as well as low Reynolds number (6.6×10^4, based on model height), and so the results are questionable in terms of applicability to full-scale structures. However, the data are useful in illustrating the strong effect of length/span ratio (L/S) on the mean pressures near the crest of the roofs. In this study the effects of lengthening the cross-section to produce a 'flat-top', and shortening it to produce a 'ridge', were also investigated. The latter modification has a particularly strong effect in modifying the mean pressure distribution over the roof.

Cook (1990), as well as describing the measurements of Toy and Tahouri in some detail, also discusses some work carried out by Blessmann (1987a, b), on arched roofs mounted on flat vertical walls. It is suggested that flow separations occur at the eave when the roof pitch angle there is less than about 30 degrees.

In a computational study of mean wind pressures (Paterson and Holmes, 1993), eleven separate geometrical configurations were examined. Figures 10.5 and 10.6 show the computed mean external pressure coefficients on a building with a rise/span ratio (R/S) of 0.2, a length/span ratio (L/S) of 1.0, and a height to eaves/rise ratio (h_e/R) 0.45, for wind directions of 0 and 45 degrees from the normal to the axis of the arch. Because of symmetry, values on one half only are shown for the 0 degree case.

For the 0 degree direction, positive pressure coefficients occur on the windward wall and the windward edge of the roof, with negative values over the rest of the structure. The highest magnitude negative values occur just upwind of the apex to the roof.

At a wind direction of 45 degrees, positive pressures only occur near the windward corner of the building. The negative pressures on the roof and walls are generally higher than those obtained for the 0 degree case, with particularly high suctions occuring along the windward end of the arch roof.

The effect of rise/span ratio is illustrated in Figure 10.7. The rise/span ratio of the building in this Figure is 0.50, compared with the building in Figures 10.5 and 10.6, which

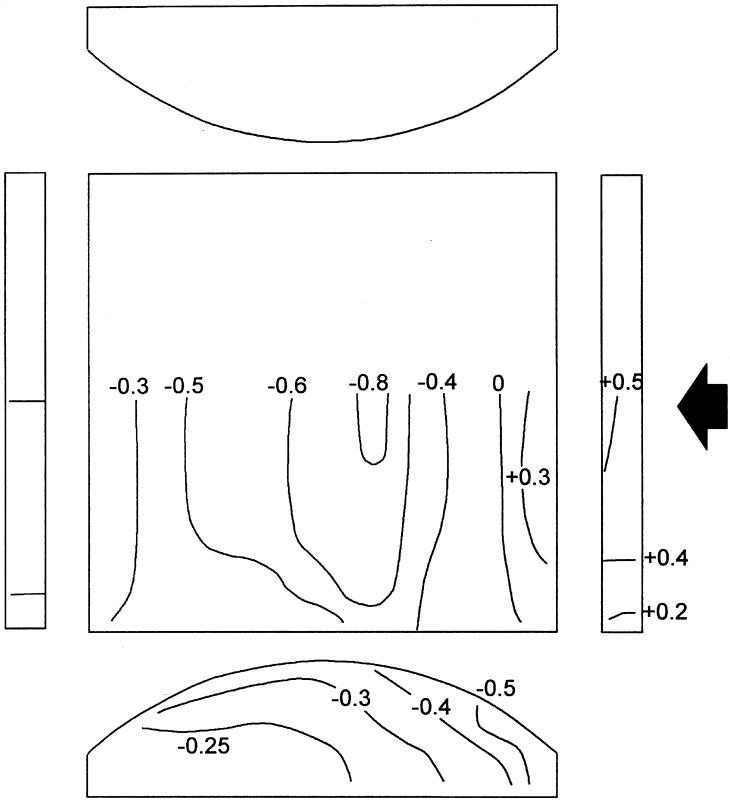

Figure 10.5 Mean pressure coefficients on an arched roof building – 0 degrees (rise/span = 0.2) (Paterson and Holmes, 1993).

has a rise/span of 0.20. It should be noted that the reference dynamic pressure ($\frac{1}{2}\rho_a \bar{U}_h^2$) is taken as the apex height of the structure in both cases, so that for a fixed span and wall height, the reference dynamic pressure will increase with increasing rise/span ratio.

As for high pitch gable roofs (Figure 8.6) there is a region of positive pressure on the windward side of the roof.

The effect of increasing length/span ratio is to increase the magnitude of both the positive and negative pressures in the central part of the building as the flow becomes more two dimensional. Increasing wall height to rise ratio (h_e/R) produces more negative values of external pressure coefficient on the roof, side walls and leeward wall (Paterson and Holmes, 1993).

For wind directions parallel to the axis of the arch, arched roofs are aerodynamically flat, with similar pressure distributions as gable roofs, for the same wind direction.

Domed roofs have similar pressure distributions as those on arched roofs, of the same rise/span ratio, for a wind direction normal to the axis.

Values of pressure coefficients for arched and domed buildings, specified in several wind loading codes and standards, are discussed in Chapter 15.

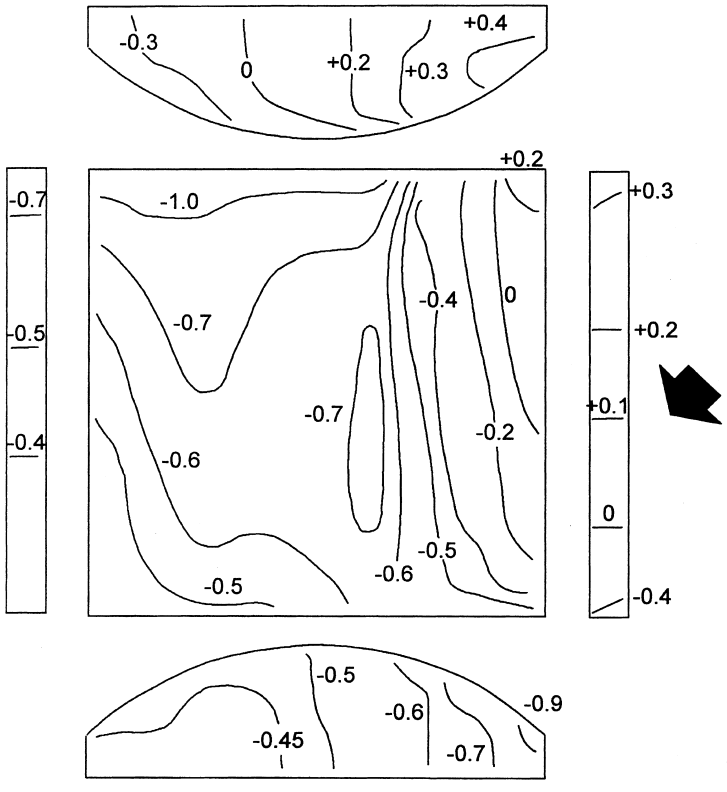

Figure 10.6 Mean pressure coefficients on an arched roof building – 45 degrees (rise/span = 0.2) (Paterson and Holmes, 1993).

10.4 Effective static load distributions

Because of the large fluctuating component in the wind loading on large roofs, the statistical correlation between pressures separated by large distances can be quite small. Designers can make use of this, to the advantage of the cost of the structure, by determining effective static load distributions. This approach enables realistic and economical design wind load distributions to be obtained using wind-tunnel tests. Two methods are possible:

- A direct approach in which simultaneous time histories of fluctuating pressures from the whole roof are recorded and stored. These are subsequently weighted with structural influence coefficients to obtain time histories of load effects. The instantaneous pressure distributions coinciding with peak load effects are then identified and averaged
- In the other approach, correlations between pressure fluctuations at different parts of the roof are obtained, and expected pressure distributions corresponding to peak load effects are obtained using methods discussed in Chapter 5.

The effective static load distribution method, discussed in Section 5.4, tries to simplify the complex time and space variation of wind pressures on structures (produced by upwind

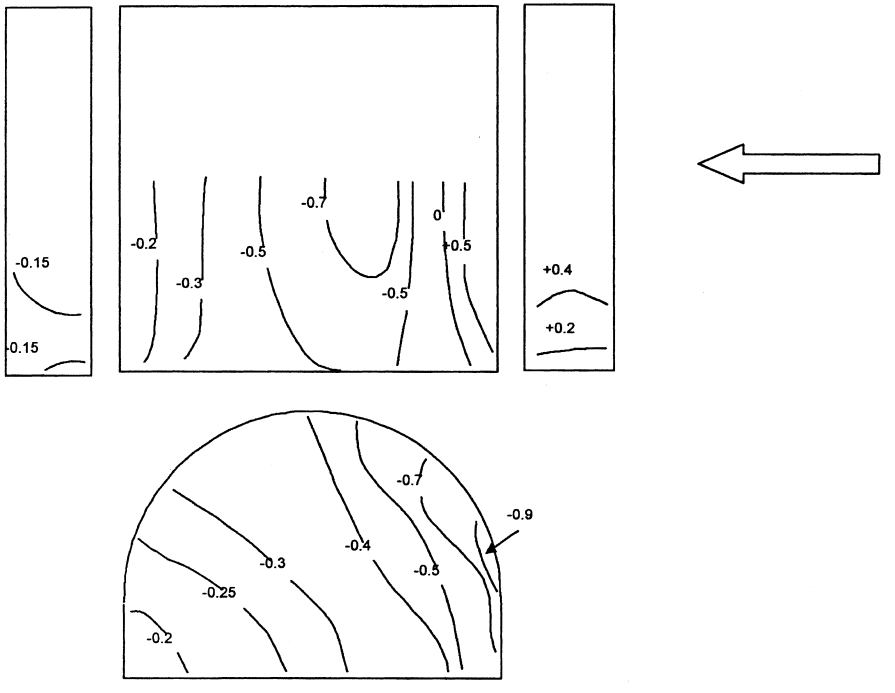

Figure 10.7 Mean pressure coefficients on an arched roof building (rise/span = 0.5) (Paterson and Holmes, 1993).

turbulence and local building-induced effects) into a number of effective static pressure distributions for structural design. It is a particularly appropriate method for large roofs, over which the pressure fluctuations are not strongly correlated (or statistically related to each other). Significant reductions in design load effects, such as axial forces and bending moments in major structural members, can be obtained by this method, although, normally wind tunnel tests are required to obtain the necessary statistical data.

The principles behind the method as applied to large roofs are illustrated in Figure 10.8. In this Figure, a section through a large arched roof is shown and the instantaneous external

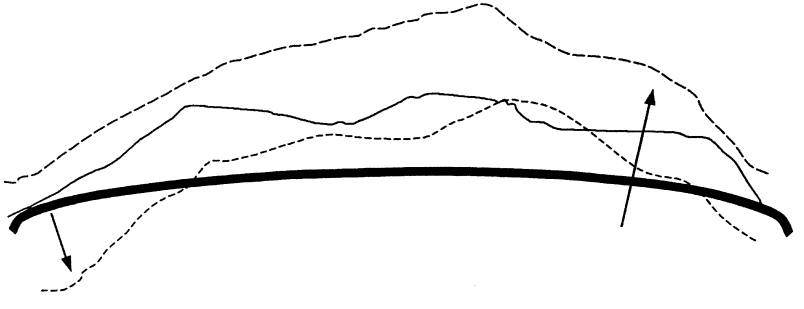

Figure 10.8 Instantaneous pressure distributions at three different times.

pressure distributions at three different points in time are shown. Clearly, there are considerable variations from time to time in these loadings. The variations are due to turbulence in the approaching wind flow, and local effects such as vortex shedding at the leading edge of the roof. The mean pressure distribution indicates only the average pressure at each point, but this distribution usually forms the basis for the design distributions of pressure found in codes. However, the instantaneous pressure distributions producing the largest load effects, may be quite different in shape to the mean.

The question of interest to the structural engineer is: what are the critical instantaneous distributions which produce the largest structural load effects in the structure? The maximum and minimum values of each load effect will be produced by two particular expected instantaneous pressure distributions, which can be determined. The main factors determining these distributions are:

- the influence line for the load effect – an example of the influence line for a bending moment in an arch is given in Figure 5.8, and
- the correlation properties of the wind pressures acting on the roof (both internal and external).

The influence lines can be calculated by the structural engineer, by applying point loads in a static structural analysis, and the correlation information can be obtained easily from wind tunnel tests.

The effective static loading distributions for the various load effects of interest can be obtained by the formula developed by Kasperski and Niemann (1992) (see also Kasperski, 1992). Examples of two of these distributions are given in Figure 5.9 in Chapter 5. The distributions for a support reaction and a bending moment are shown. Clearly these two distributions differ considerably from each other, due to the different influence lines for the two load effects. They also differ from the mean pressure distribution. The shaded area in Figure 5.9 indicates the limits of the instantaneous maximum and minimum peak pressures around the arch, which form an 'envelope' within which the effective static loading distributions must fall.

When applying the effective static wind-load distribution approach to large roofs, usually a limited number of load effects are considered and effective static load distributions are computed for them. These are then 'enveloped' to give a smaller number of wind pressure distributions, which are then used by the structural engineers to design all the members of the structure. If required by structural designers, the peak values of critical load effects, such as forces in main members, or deflections can be directly computed.

10.4.1 Contributions of resonant components

When considering dynamic response of any structure to wind, it is necessary to distinguish between the resonant response at or near the natural frequencies of the structure, and the fluctuating response at frequencies below the first or lowest frequency, or 'background response', which is usually the largest contributor. As for all structures, the significance of resonant dynamic response to wind for large roofs, depends on the natural frequencies of vibration, which are in turn dependent on the mass (inertia) and stiffness properties, and the damping. For roofs which are supported on two or four sides in the case of a rectangular plan, or all the way round in the case of a circular plan, the stiffness is usually high enough that resonant response is very small and can be ignored. For totally enclosed buildings, additional stiffness is provided by compression of the air inside the building.

Also there is additional positive aerodynamic damping which further acts to mitigate any resonant dynamic response.

Extra large stadium roofs may have several natural frequencies below 1 Hz, although these can be expected to have quite high damping.

Roofs supported on one side only, i.e. cantilevered roofs, however, are more prone to significant resonant response due to the lower stiffness. Figure 10.9 shows some resonant response in the time history of vertical deflection at the leading edge of a model cantilevered roof in wind tunnel tests. The use of stiffening cables often increases the stiffness sufficiently to reduce the resonant contribution to minor proportions.

Most codes and standards do not include the effects of resonant response on large roofs – the Australian Standard AS1170.2 (Standards Australia, 1989) is an exception – it contains a design load distribution which is dependent on natural frequency.

If resonant response is anticipated to be substantial on a large roof, wind tunnel testing with an aeroelastic model is often recommended. These can be very useful but have limitations, in that accurate effective load distributions cannot be determined from them, and the structural stiffness cannot be altered to accommodate design changes once the model has been built. For important structures, a rigid pressure model test is also advisable to obtain the distributions in pressure for the mean and background components, as discussed earlier. The resonant response can also be computed from the spectra and cross-spectra of the fluctuating pressures at the natural frequency, or from the time histories of the generalised forces in the contributing modes of vibration. Either method is computationally complex and requires simultaneous pressure measurement over the entire roof (including the underside pressure for an open stadium roof), but this is certainly feasible and has been used for large projects at wind tunnel laboratories in Australia and elsewhere.

Usually the resonant response will comprise no more than 10 to 20% of the peak values of critical load effects (Holmes *et al*., 1997), and this contribution can be calculated separately and added to the fluctuating background response using a 'root-sum-of-squares approach'. The effective static load distribution corresponding to each peak load effect can then scaled up to match the recalculated peak load effect.

For very large roofs several resonant modes can contribute, and the evaluation of effective static loads becomes more difficult. In general it is necessary to adopt the approach of Section 5.3.7 in which the background response is separated from the resonant components, as these components all have different loading distributions. The magnitude of the contribution from each resonant mode depends on the load effect through its influence line. Section 12.3.4 describes the application of the equivalent static load approach to

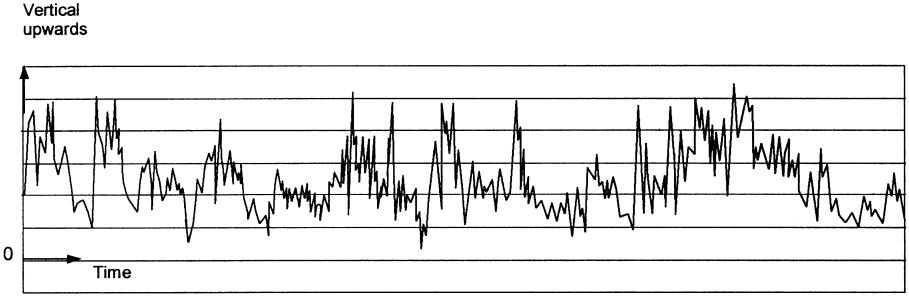

Figure 10.9 Vertical displacement of the leading edge of a cantilevered roof showing some resonant contributions to the response (Melbourne, 1995).

long-span bridges, when more than one resonant mode contributes. This approach can also be applied to very large roofs; in this case the background contribution is treated as an additional 'mode', for which the effective load distribution is calculated separately.

Thus the effective static load distribution for the combined background and resonant contributions is:

$$p'_{eff}(x) = W'_B.p_{eff,back}(x) + \sum_{j}^{N} W'_j m(x)\phi_j(x) \tag{10.1}$$

where the weighting factors are given by:

$$W'_B = \frac{\sigma_{r,B}}{\left\{\sigma_{r,B}{}^2 + \sum_{j=1}^{N} \alpha_j{}^2 \omega_j{}^4 \overline{a_j^2}\right\}^{1/2}} \tag{10.2}$$

$$W'_j = \frac{\alpha_j \omega_j{}^4 \overline{a_j^2}}{\left\{\sigma_{r,B}{}^2 + \sum_{j=1}^{N} \alpha_j{}^2 \omega_j{}^4 \overline{a_j^2}\right\}^{1/2}} \tag{10.3}$$

where $\sigma_{r,B}$ is the background component of the load effect, and the other terms are defined in Section 12.3.4. The derivation of the background effective static load distribution, $p_{eff,back}(x)$ is described in Chapter 5.

10.5 Wind tunnel methods

As discussed in previous sections, large roofs are usually dominated by the mean wind pressures and the background fluctuating components. Resonant contributions to the wind-induced structural load effects are usually small, even though natural frequencies as low as 0.5 Hz can occur for the largest roofs. The main reason for this behaviour is the nature of the separating–re-attaching flow over large roofs of low pitch, and the consequent very low correlations between fluctuating pressures acting on different parts of the roof. Excitation of a dynamic mode requires pressure 'modes' which are coincident with the mode shape, at the modal frequency in question. Usually the excitation energy satisfying these conditions is small. Another reason for low resonant response is high damping with significant positive contributions from aerodynamic damping (Section 5.5.1).

For the reasons given above, modern wind tunnel testing of large roofs for sports stadiums or arenas, is usually carried out with rigid models on which detailed pressure measurements are made. The techniques used are described in Section 7.6.6. Using recorded time histories of fluctuating pressures, computations can be made of the resonant contributions, and added to the mean and background fluctuating contributions.

Full aeroelastic models of large roofs, although used quite frequently in the past, are now much less common. They are quite expensive to design and build, are structure-dependent, and do not lend themselves to changes in the underlying structure during the design process. Also they can only normally be used for deflection measurements. However for very flexible cantilevered roofs, the use of aeroelastic models may be required in conjunction with tests on rigid models.

10.6 Test cases

The effective static wind-load distribution method (Section 10.4), based on measurement of correlations between fluctuating pressures on panels on different parts of the roof, as applied in conjunction with wind tunnel tests, to two large stadium roofs is described by Holmes *et al.* (1997). This reference also discusses the effects of resonant load components. Some results from that study are given in Figure 10.10.

The alternative approach, based on the direct weighting of the recorded fluctuating pressures by influence coefficients, is described by Xie (2000). This is a case study of a stadium roof consisting of two large cantilevered panels with a complex curvature.

10.7 Summary

This chapter has attempted to cover the main aspects of wind loads on large roofs, including those used increasingly for sports stadiums. The characteristics of airflow and mean

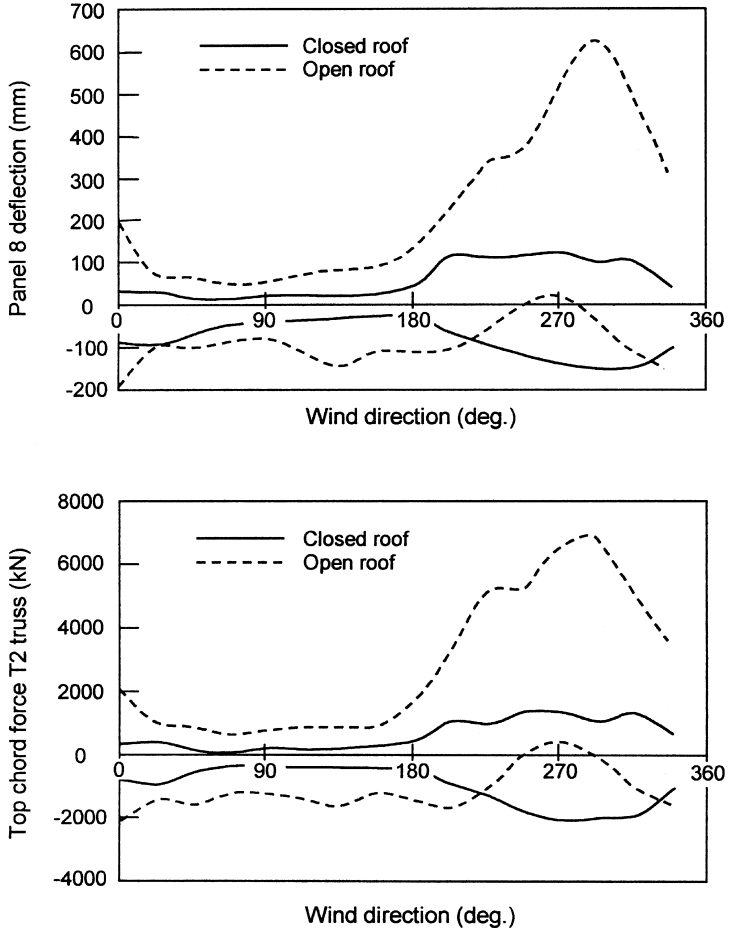

Figure 10.10 Variation of a deflection and a main truss force for a large stadium roof computed from a wind tunnel pressure model test (from Holmes *et al.*, 1997).

pressure distributions on flat, arched and domed roofs are discussed. There is some overlap with Chapter 8 'Low-rise Buildings', but there are some significant differences – namely the large effects of the reduced correlations between fluctuating pressures over large expanses of low-pitch roofs, and the possibility of some resonant response contributions.

The application of wind tunnel methods, using pressure measurements on rigid models, to the determination of effective static wind-load distributions is discussed.

References

American Society of Civil Engineers (1936) 'Wind-bracing in steel buildings', Fifth Progress Report of Sub-Committee No. 31. *Proceedings A.S.C.E.,* March 1936, 397–412.

Arnstein, K. and Klemperer, W. (1936) 'Wind pressures on the Akron Airship-dock', *Journal of the Aeronautical Sciences*, 3: 88–90.

Blessmann, J. (1987a) 'Acao do vento em coberturas curvas, la Parte', Caderno Tecnico CT-86. Universidade Federale do Rio Grande do Sul.

—— (1987b) 'Vento em coberturas curvas – pavilhoes vizinhos', Caderno Tecnico CT-88. Universidade Federale do Rio Grande do Sul.

—— (1991) 'Acao do vento em telhados', SAGRA, Porto Alegre, Brazil.

Bounkin, A. and Tcheremoukhin, A. (1928) 'Wind pressures on roofs of buildings', Transactions, Central Aero- and Hydrodynamical Institute, Moscow, No. 35.

Cook, N. J. (1990) *The Designer's Guide to Wind Loading of Building Structures. Part. 2. Static Structures*. Building Research Establishment (U.K.).

Davenport, A. G. and Surry, D. (1974) 'The pressures on low-rise structures in turbulent wind', *Canadian Structural Engineering Conference,* Toronto.

Grillaud, G. (1981) 'Effet du vent sur une structure gonflable', *Colloque, 'Construire avec le Vent'*, Nantes, France, June.

Holmes, J. D. (1984) 'Determination of wind loads for an arch roof', *Civil Engineering Transactions, Institution of Engineers, Australia* CE26: 247–53.

Holmes, J. D., Denoon, R. O., Kwok, K. C. S. and Glanville, M. J. (1997) 'Wind loading and response of large stadium roofs', *Proceedings, IASS International Symposium '97 on Shell and Spatial Structures*, Singapore, 10–14 November.

Hoxey, R. and Richardson, G. M. (1983) 'Wind loads on film plastic greenhouses', *Journal of Wind Engineering and Industrial Aerodynamics* 11: 225–37.

Kasperski, M. (1992) 'Extreme wind load distributions for linear and nonlinear design', *Engineering Structures* 14: 27–34.

Kasperski, M. and Niemann, H.-J. (1992) 'The L.R.C. (Load-Response-Correlation) method: a general method of estimating unfavourable wind load distributions for linear and non-linear structural behaviour', *Journal of Wind Engineering Industrial Aerodynamics* 43: 1753–63.

Johnson, G. L., Surry, D., and Ng, W. K. (1985) 'Turbulent wind loads on arch-roof structures: a review of model and full-scale results and the effect of Reynolds Number', *5th U.S. National Conference on Wind Engineering*, Lubbock, Texas, November 6–8.

Lam, K. M. and To, A. P. (1995) 'Generation of wind loads on a horizontal grandstand roof of large aspect ratio', *Journal of Wind Engineering and Industrial Aerodynamics* 54/55: 345–57.

Melbourne, W. H. (1995) 'The response of large roofs to wind action', *Journal of Wind Engineering and Industrial Aerodynamics* 54/55: 325–35.

Paterson, D. A. and Holmes, J. D. (1993) 'Mean wind pressures on arched-roof buildings by computation', *Journal of Wind Engineering and Industrial Aerodynamics* 50: 235–43.

Standards Australia (1989) *Minimum Design Loads on Structures. Part 2: Wind Loads*. Standards Australia, North Sydney, Australian Standard AS1170.2-1989.

Toy, N. and Tahouri, B. (1988) 'Pressure distributions on semi-cylindrical structures of different geometrical cross-sections', *Journal of Wind Engineering and Industrial Aerodynamics* 29: 263–72.

Xie, J. (2000) 'Gust factors for wind loads on large roofs', *First International Symposium on Wind and Structures*, Cheju, Korea, January.